1 **Behavioural and transcriptomic characterization of the comorbidity between**
2 **Alzheimer's disease and Major Depression**

3 Ana Martín-Sánchez[1], Janet Piñero[2], Lara Nonell[2,3], Magdalena Arnal[2], Elena M. Ribe[4], Alejo
4 Nevado-Holgado[4,5], Simon Lovestone[4,6], Ferran Sanz[2], Laura I. Furlong[2], Olga Valverde[1*]
5
6 [1.] Neurobiology of Behaviour Research Group (GReNeC-NeuroBio), Department of
7 Experimental and Health Sciences, Universitat Pompeu Fabra; Neuroscience Research Program,
8 IMIM-Hospital del Mar Research Institute, Barcelona, Spain.
9 [2.] Research Programme on Biomedical Informatics (GRIB), IMIM (Hospital del Mar Medical
10 Research Institute), Universitat Pompeu Fabra, Barcelona, Spain.
11 [3.] MARGenomics core facility, IMIM (Hospital del Mar Medical Research Institute), Barcelona,
12 Spain.
13 [4.] Department of Psychiatry, University of Oxford, Oxford OX3 7JX, UK
14 [5.] Oxford Health NHS Foundation Trust, Oxford OX3 7JX, UK
15 [6] currently at Janssen-Cilag, UK
16
17 [*]Correspondence should be addressed to:
18 Olga Valverde
19 Department of Experimental and Health Sciences (DCEXS)
20 Universitat Pompeu Fabra
21 Carrer Doctor Aiguader 88, Barcelona 08003 Spain
22 Tel: +34 93 316 08 67
23 E-mail: olga.valverde@upf.edu

24 **ABSTRACT**

25 Major Depression (MD) is the most prevalent psychiatric disease in the population and is
26 considered a prodromal stage of the Alzheimer's disease (AD). Despite both diseases having a
27 robust genetic component, the common transcriptomic signature remains unknown. In this regard,
28 we investigated the cognitive and emotional responses in 3- and 6-month-old in APP/PSEN1-Tg
29 mutant mice, before β-amyloid plaques were detected. Then, we studied the deregulation of genes
30 and pathways in prefrontal cortex, striatum, hippocampus and amygdala, using transcriptomic
31 and functional data analysis. The results demonstrated that depressive-like and anxiety-like
32 behaviours, as well as memory impairments are already present at 3-month-old together with the
33 deregulation of several genes and gene sets, including components of the circadian rhythms,
34 electronic transport chain and neurotransmission. Finally, DisGeNET GSEA provides
35 translational support for common depregulated gene sets related to MD and AD. Altogether, the
36 results demonstrate that MD could be an early manifestation of AD.

37 **ABBREVIATIONS**

AD	Alzheimer's disease
APP	Beta-Amyloid precursor protein
BSPD	Behavioural and psychological symptoms of dementia
DE	Differential expression

EPM	Elevated plus maze
FC	Fold change
FDR	False discovery rate
GSEA	Gene set enrichment analysis
GWAS	Genome-wide association study
ICD-9	International Classification of Diseases, 9th Edition
MD	Major Depression
NES	Normalized enrichment score
NOR	Novel object recognition
OF	Open field
PFC	Prefrontal cortex
PSEN1	Presenilin-1
TST	Tail suspension test

38

INTRODUCTION

Depressive disorder affects over 4.4% of the population[1], and it is characterized by feelings of sadness, anhedonic state, changes in appetite and sleep, feelings of worthlessness, guilt, and may lead to attempts of suicide[1]. Major Depression (MD) manifests throughout the life course. In older people it is often associated with poor cognition that may not return to normality with effective treatment of the mood disorder[2,3]. In addition to the cognitive phenotype of MD in older people, a substantial body of data strongly suggests onset of MD in later life is associated with increased risk of Alzheimer's disease (AD), the commonest form of dementia[4–6]. Furthermore, although cognitive and functional impairments are the predominant symptoms of AD, other behavioural and psychological symptoms of dementia (BPSD) that include depression, sleep and activity disturbance are common manifestations of the disease[7,8]. These observations have led to the suggestion that MD may in some cases be a prodromal phase of AD. Indeed, both MD and AD have a considerable heritable component and share some mechanistic components including neuroinflammation[9,10], oxidative stress[11], certain dysregulations in cellular signalling[12] and neurotransmission[13,14] amongst others.

Despite these advances, the aetiology of the comorbidity between AD and MD remains unknown although the observation that multiple behaviours that are reminiscent of BPSD are also observed in rodent models of disease[15] suggesting that there might have common molecular processes. Hereby, we study for the first time, using behavioural, transcriptomic and bioinformatic approaches, depressive-like symptoms in an AD mouse model (APP/PSEN1-Tg mice) at ages before the neuropathological features are manifest and when cognitive impairment is not evident[16]. To that end, we have performed RNA sequencing analyses to study changes that occur in brain areas related to the control of behavioural and cognitive behaviours, including prefrontal cortex (PFC), striatum, hippocampus and amygdala, in mice at 3 and 6 months old. In order to study the mechanisms involved in the AD-MD comorbidity, a pre-ranked Gene Set Enrichment Analysis (GSEA) has been carried out. Using the transcriptomic results, we evaluated the enrichment in genes sets obtained from public resources containing functional and disease information.

RESULTS

The transgenic mice expressing human APP/PSEN1-Tg carrying familial AD mutations used in these studies (B6C3-Tg) have an onset of plaque pathology at around 6 months, which is followed by cognitive impairments with both increasing by 12-15 months of age. To explore behavioural alterations in these mice, we used a range of well-established experimental paradigms at 3 months (before the onset of pathology) and 6 months (at onset). Then, we evaluated the

73   differentially expressed genes and pathways in PFC, striatum, hippocampus and amygdala at both
74   ages.

Anxiety-related behaviour in APP/PSEN1-Tg mice

76   To evaluate if APP/PSEN1-Tg animals experience anxiety-like behaviour, 3 and 6-
77   month-old APP/PSEN1-Tg were subjected to the elevated plus maze (EPM). The APP/PSEN1-
78   Tg transgenic mice spent lower percentage of time in open arms than Non-Transgenic at both 3
79   (t_{30}= 2.30, p=0.0286; Figure 1A) and 6 months old (t_{26}=2.419, p=0.0229; Figure 1D), whereas no
80   differences were found in the total number of arm entries (t_{30}= 0.65, p=0.520, Figure 1B and
81   t_{26}=1.21, p=0.236, Figure 1E), indicating that APP/PSEN1-Tg animals displayed higher level of
82   anxiety-like behaviours without locomotor impairments.

Early onset of despair-like behaviour in APP/PSEN1-Tg mutant mice

84   Stress induced immobility is a despair responsive phenotype often used as a proxy for
85   mood state in rodent models. To evaluate this response, we performed the tail suspension (TST)
86   in APP/PSEN1-Tg transgenic and control mice.

87   At 3 months old, the analysis of the TST results using an ANOVA for repeated
88   measurements revealed *stress* ($F_{1,30}$ =20.77, p<0.001), *genotype* ($F_{1,30}$=5.27, p=0.029) and
89   *stress×genotype* ($F_{1,30}$=8.61, p=0.006; Figure 1 C) effects. After Bonferroni's correction, results
90   showed that transgenic mice presented higher stress-induced immobility (p<0.001) in comparison
91   with the pre-stress condition. Stress only increased the percentage of the immobility in
92   APP/PSEN1-Tg mutants in comparison with Non-Transgenic animals (p=0.005).

93   At 6 months, the ANOVA for repeated measurements showed *stress* ($F_{1,24}$ =31.33,
94   p<0.001) and *genotype* ($F_{1,24}$=4.62, p=0.042; Figure 1F) effects. These results indicate that
95   transgenic mice spent a higher percentage of immobility time and after repeated stress, but also
96   this behaviour increases in both groups of mice.

Early-adulthood long-term memory impairments in APP/PSEN1-Tg mice

98   Loss of memory is affected early during the time-course of the AD, being one of the most
99   recognizable symptoms of the disease[17]. For this reason, we assessed the short- and long-term
100   recognition memory in 3- and 6-month-old APP/PSEN1-Tg mice using the novel object
101   recognition test.

102   At 3 months old, a two-way ANOVA showed a *genotype* ($F_{1,29}$=8.30, p=0.007), and
103 *object* effect ($F_{1,29}$=36.93, p=0.001; Figure 2A). The *genotype* effect indicates that control animals
104 had greater discrimination index than APP/PSEN1-Tg group.

105   At 6 months, a two-way ANOVA revealed a main effect of *genotype* ($F_{1,24}$=22.44,
106 p<0.001), an *object* effect ($F_{1,24}$=6.51, p=0.018) and *object × genotype* interaction ($F_{1,24}$=14.64,
107 p=0.001; Figure 2D). The *genotype* effect shows that control animals had greater discrimination
108 index than transgenic mice. The *post-hoc* Bonferroni's analysis showed that Non-Transgenic
109 mice could discriminate both the novel object 1 and 2 in the same manner (p=0.394), whereas
110 APP/PSEN1-Tg animals could only discriminate novel object 1, having a greater discrimination
111 index for the novel object 1 than novel object 2 (p<0.001). Non-Transgenic animals had higher
112 discrimination index than APP/PSEN1 when they are exposed to novel object 2 (p<0.001). In fact,
113 APP/PSEN1-Tg animals could not discriminate between familial and novel object 2, indicating
114 important memory impairments.

115 *Early poor left-right discrimination learning of APP/PSEN1-Tg mice*

116   In order to evaluate working memory and attention deficits present in AD[18], we performed
117 a left-right discrimination learning paradigm in 3 and 6 month APP/PSEN1-Tg transgenic and
118 Non-Transgenic mice using the T-maze.

119   The two-way ANOVA showed a *trial* effect ($F_{9,270}$= 2.152, p=0.026) and *trial × genotype*
120 ($F_{9,270}$=2.023 p=0.037; Figure 2B) at 3 months old. The *post-hoc* analysis revealed that
121 APP/PSEN1-Tg animals took more time to reach de platform than control animals on trial 1
122 (p=0.044) and trial 5 (p=0.027) during the acquisition learning. However, this analysis suggests
123 that control mice spent more time to reach the platform during the trial 2 of the reversal-learning
124 phase (p=0.02) than transgenic mice. The pair-wise comparison showed that APP/PSEN1-Tg
125 reduced the time to escape on acquisition trial 2 (p=0.037) and trial 2 of the reversal learning
126 (p=0.017) in comparison with the trial 1 of the acquisition. We found that APP/PSEN1-Tg
127 animals spent more trials than Non-Transgenic animals (t_{30}=2.35, p=0.026; Figure 2C) to reach
128 the acquisition criterion. Nevertheless, both groups spent a similar number of trials to reach the
129 criteria during reversal learning (p=0.443).

130   At 6 months old, the ANOVA revealed a *trial* ($F_{9,216}$= 3.84, p<0.001) and *genotype*
131 ($F_{1,24}$=6.53, p=0.017, Figure 2E) effects, suggesting that APP/PSEN1-Tg mutant mice showed
132 longer latencies to reach the platform than control animals during acquisition and reversal
133 learning phases. The mean latency to get the acquisition criteria showed a trend to be statistically

134 different in the number of trials that APP/PSEN1-Tg in comparison with control mice (t_{24}=1.91;

135 p=0.068; Figure 2F).

136 *Hyposmia in APP/PSEN1-Tg mice at 6 months old*

137 Since olfactory impairment is present in up to 90% of AD patients[19], we assessed the

138 olfactory function in transgenic and control mice (Figure 3A and C).

139 At 3 months old, both experimental groups could discriminate between the first water

140 presentation and limonene odour (Wilcoxon test, Non-Transgenic group, p=0.05 and

141 APP/PSEN1-Tg, p=0.01; Figure 3A).

142 At 6 months, both APP/PSEN1-Tg transgenic mice and Non-Transgenic mice could

143 discriminate between the first water presentation and limonene (Wilcoxon test, Non-Transgenic,

144 p=0.006, and APP/PSEN1-Tg, p=0.008; Figure 3C). Additionally, APP/PSEN1-Tg mutant mice

145 showed a higher investigation time during the fifth water presentation than control group

146 (Kruskal-Wallis test, χ^2=3.84, p=0.05; Figure 3C). Whereas both experimental groups spent the

147 same time investigating the cotton swab at 3 months old (t_{22}=0.66, p=0.52; Figure 3B),

148 APP/PSEN1-Tg mutant increased the investigation time than Non-Transgenic control animals,

149 showing an indiscriminate investigation at 6 months-old (t_{21}=2.52, p=0.02; Figure 3D),

150 independently of the type of odour presented.

151 *DE analysis in PFC, striatum, hippocampus and amygdala at two different ages*

152 We performed gene expression analysis in regions of the brain known to be loci for these

153 functions. We compared the transcriptome signature of APP/PSEN1-Tg transgenic and control

154 mice at 3 and 6 months old, to determine the significant differentially expressed (DE) genes with

155 a cut-off |logFC | < 0.585, adjusted p<0.05, deregulated in the brain areas of interest (Figure 4;

156 Supplementary Tables 2-5).

157 Among the dysregulated genes in PFC of younger APP/PSEN1-Tg mice, we found 5

158 corresponding to the so-called canonical clock genes: *Ciart*, *Dbp*, *Bhleh41* and *Nr1d1* were

159 downregulated, and *Nfil3* was upregulated, together with other genes, such as *App*, *Prpn*, *Inhba,*

160 and *Fosl2* (Figure 4A; Supplementary Table 2). At 6 months-old mice, *Dbp* and *Nr1d1* remained

161 downregulated in this area, whereas *App*, *Prnp* were also upregulated together with *Itgax* and

162 *Maml3* (Figure 4B; Supplementary Table 2).

163 In the striatum of 3-months-old mice, we only found the downregulation of *Ciart,* and the

164 overexpression of *App*, *Prpn* and *Edn1* (Figure 4C; Supplementary Table 3). By contrast, the

165   deregulation of older mice in the striatum was restricted to only one downregulated transcript,

166   *RP23-152P11.2*, whilst *App* and *Prpn* remained upregulated (Figure 4D; Supplementary Table

167   3).

168   In the hippocampus of 3-months-old APP/PSEN1-Tg mice, 8 genes were downregulated,

169   including *Ptx4* and *Mc4r* and *Zap70*. Among the upregulated genes, we found *Plch1*, *Cdh23*,

170   *Itga10*, *App*, *Prnp*, and *Inhba* (Figure 4E; Supplementary Table 4). At 6 months, the analysis

171   revealed that only *App* and *Prnp* remained upregulated (Figure 4F; Supplementary Table 4).

172   Interestingly, the amygdala of young transgenic mice was the most affected structure.

173   More than 100 genes were upregulated in the amygdala of the 3-month-old AD mice (Figure 5A;

174   Supplementary Table 5), including *Tnfαip8l3*, *Sstr1*, *Sstr4*, *Chrm5* and *Aldh1a3* (Figure 4G;

175   Figure 5A and C). Among the almost 100 downregulated genes in the amygdala at 3 months old

176   (Figure 4G; Supplementary Table 5), we found *Grin3b*, *Chrna10* and *Ciart*. However, when we

177   analysed the number of deregulated genes at 6 months old, both the upregulated and

178   downregulated genes dramatically decreased in all brain areas (Figure 4H, Figure 5B). In

179   amygdala, the upregulation of genes diminished to three genes, *App*, *Prnp* and *Clec7a* (Figure

180   4H, Figure 5B, D) while the downregulated genes were restricted to *Dbp* and *Ciart* (Figure 4H;

181   Figure 5C, H).

182   When we compared those genes that were consistently deregulated at both ages per area,

183   we observed that the upregulation of *App* and *Prnp* were extended throughout PFC, hippocampus

184   and amygdala (Figure 4A,E,G; Figure 5E). Moreover, this upregulation at 6 months-old was

185   affecting all brain regions Figure 4B,D,F and H; Figure 5E). By contrast, *Ciart* was

186   downregulated in PFC, striatum, and amygdala of APP/PSEN1-Tg mice at 3 months old. Only

187   *Nr1d1*, *Dbp* in PFC and *Dbp* and *Ciart* in amygdala were downregulated in the older transgenic

188   mice (Figure 4B,H; Figure 5H).

189   *Enriched gene sets at 3 and 6 months-old*

190   We then performed bioinformatic analyses to determine pathways altered in the

191   transgenic mice in the pre-disease and early pathology periods (3 months and 6 months). This

192   functional analysis showed enriched gene sets related to depressive disorders appear at 3 month-

193   old within PFC, hippocampus and amygdala, areas that are intimately involved in both cognitive

194   function and mood regulation (Figure 6A,B,D and E; Supplementary Table 6). In the striatum,

195   we only identified two positively enriched gene sets - those of circadian rhythms and Alzheimer's

196   disease (Figure 6C) - that also appear in PFC, hippocampus and amygdala at early stages. In the

197   6 months-old animals, however, the number of gene sets that were significantly enriched in

198   APP/PSEN1-Tg transgenic mice was higher. We identified additional negatively enriched

199   pathways linked to the electron transport chain, found in the PFC, striatum and hippocampus

200   (Figure 6F, G and H; Supplementary Table 7) and also pathways implicated in AD and

201   neuroinflammation. In parallel, the positively enriched depressive-related gene sets not only

202   increased in number but also the dysregulation of these pathways extended to all the brain

203   structures analysed (Figure 6F-I) at this later age. Additionally, the neurotransmission-related

204   pathways were more enriched in 6-month-old transgenic mice than at early ages, suggesting that

205   neurodegeneration increased the number of affected gene sets. By contrast, the impairments in

206   circadian rhythms seem to appear in the preclinical phase in the amygdala (Figure 6B-E),

207   persisting at least to the period when pathology becomes apparent (Figure 6I).

208   We then extended these findings to human data by performing GSEA analysis using

209   DisGeNET (version v7.0; http://www.disgenet.org/) gene sets (Supplementary Figure 3;

210   Supplementary Tables 8 and 9). DisGeNET is a knowledge resource that collects information

211   about the genetic underpinnings of human diseases. This GSEA, which is specific for diseases

212   and disease-related phenotypes, showed positively enriched gene sets corresponding to several

213   subtypes of AD and dementias in the PFC and hippocampus of 3-month-old animals.

214   Additionally, we found positively enriched gene sets associated with memory impairment

215   phenotypes, anxiety disorders, traits and symptoms related to motor impairment, and to

216   neurodegenerative diseases in the hippocampus of younger animals. These results are consistent

217   with the deregulated pathways shown in Figure 6 and with the results of the behavioral tests. In

218   6-month-old animals, the DisGeNET GSEA showed that positively enriched gene sets of several

219   subtypes of AD and dementias and those related to memory impairment were extended to all brain

220   areas. This dysregulation of processes related to memory impairment in old animals is consistent

221   with the working memory deficits and learning impairments that displayed 6-month-old animals

222   displayed in the behavioural experiments. Moreover, positively enriched gene sets related to

223   diseases of the central nervous system were observed in the hippocampus and striatum of 6-

224   month-old animals. Most of these diseases are cerebrovascular diseases, which have been related

225   to MD[20]. The connection between this class of disorders and MD have been suggested to be

226   mediated by inflammation[21], which is consistent with the dysregulation of neuroinflammation

227   pathways found in hippocampus of young and old animals (Figure 6A,D,H).

228   **DISCUSSION**

229   This study provides the first evidence of early, pre-pathological, depression-like

230   symptoms, as well as cognitive impairment, and the underpinning transcriptomic changes

231   specifically in PFC, striatum, hippocampus and amygdala in a rodent AD model (B6C3-Tg

232   (APPswe, PSEN1dD9)85Dbo/MmJax). In particular, APP/PSEN1-Tg transgenic mice show both

233   pre-pathological and peri-pathological deficits in different behaviours. On the one hand, the

234   anxiety-related behaviours and despair behaviours after stressful conditions, hyperlocomotion

235   and diminishing discrimination begins, in the model used, at 3 months of age, before the onset of

236   pathology. On the other hand, the hyposmia traits, working memory deficits and reversal learning

237   impairments appear later at 6 months old, at the time when amyloid plaque pathology begins to

238   become apparent.

239   The behavioural experiments indicate that APP/PSEN1-Tg mice showed early anxiety-

240   like and depressive-like traits, symptoms which would be expected to be associated with

241   dysfunction of the amygdaloid, hippocampal and PFC circuitries. Supporting these observations,

242   the genes *Nr1d1* and *Bhlhe41* , which have been previously associated with both control of

243   circadian rhythms function and with depression[22,23], were downregulated in the PFC of transgenic

244   mice. Moreover, *Plch1* is upregulated at 3 months old in the transgenic mice. The product of this

245   gene is part of the pathway generating second messengers, such as inositol 1,4,5-triphosphate and

246   diacylglycerol; a pathway which is intimately linked to the depressive-like phenotype[24]. At 3 but

247   not at 6 months old, we found the upregulation of *Inhba* in PFC and hippocampus, which could

248   represent a compensatory change to mitigate the depressive-like behaviour. In fact, the activin

249   signalling pathway plays a key role in the response to antidepressant treatment in humans[25]. *Nr1d1*

250   remains downregulated at 6 months old, without changes in *Inhba* signalling, due to possible

251   deeper detrimental effects at older ages, e.g. deficits in working memory. Additionally, *Mc4r* is

252   downregulated in hippocampus at 3 months old and facilitates anxiety-like and depression-like

253   behaviours pursuant to chronic stress[26]. Indeed, a general overexpression of *Prnp* and *App* in 3-

254   and 6-month-old APP/PSEN1-Tg mutant mice could also contribute to this depressive-like

255   symptomatology, since previous studies found alterations of these protein levels in cortical areas

256   and peripheral blood of MD[27,28]. Noteworthy, this mouse overexpresses APP695 containing the

257   double Swedish mutation, so the general upregulation of *App* found in all brain areas of interest

258   is directly induced by the model. Moreover, *Prnp* may modulate depressive-like behaviour in

259   mice via interactions with monoaminergic neurotransmission[29]. In accordance with these results,

260   we observed an increasing number of enriched pathways linked to depressive disorders (including

261   depression, apathy and anxiety, among others) and disease-associated gene sets at 3 and 6 months

262   old, before the period of formation of β-amyloid plaques in this model[30]. These results therefore

263   support the notion that depressive symptoms are part of the prodromal phase of the AD in this

264   rodent model, just as they are hypothesised to be in human disease.

265   Overall, the APP/PSEN1-Tg mutant mice had a general decline in memory with ageing,

266   as previously described in AD models[15,31] but these phenomenon was demonstrated before the

267   onset of pathology, although became more extensive at about the time pathology was expected.

268   Despite a subtle imbalance of memory impairment pathways at 3 months old, transgenic mice

269   showed higher latencies to acquire the criterion in the left-right discrimination test. These memory

270   deficits could be promoted by the observed dysregulation of *Cdh23*, *Ptx4* and *Mc4r* genes in

271   hippocampus, as they are known to participate in the endocytosis of glutamatergic ionotropic

272   AMPA receptors, hippocampal synaptic plasticity and mood-like disorders in mice,

273   respectively[32–35]. At 6 months old, APP/PSEN1-Tg mutant mice show deeper deficits in memory

274   in all the evaluated tasks. They display longer latencies in left-right discrimination task, and

275   deficits in working and long-term memories. These memory impairments run in parallel with an

276   increasing number enriched pathways in PFC and hippocampus (abnormal long-term spatial

277   reference and spatial memories, among others), involved in working[36,37] and spatial learning[38,39],

278   respectively, and with dysregulation of gene sets related to memory impairment and learning

279   disabilities (Supplementary Figure 3).

280   Our results show that the APP/PSEN1-Tg, at 3 months old mice spent the same time than

281   the control mice investigating the cotton-swabs, which have been impregnated with limonene.

282   However, at 6 months old the exploration of both odours was increased in transgenic mice

283   compared to the control group, independently whether water and limonene were presented.

284   Overall, APP/PSEN1-Tg animals seem not to present a complete anosmia, although it seems that

285   they display a loss of discrimination between odours, so this possible hyposmia together with

286   working memory[36,37] impairments could explain the indiscriminate investigation that transgenic

287   mice display. These olfactory alterations could be due to pathology in the olfactory bulb at 6

288   months-old[40], that might be promoting changes in the sense of smell of APP/PSEN1-Tg mice.

289   Thus, our mice model could reflect the progressive anosmia that AD patients show at early stages

290   of the disease[19]. Indeed, a recent study shows that late-depression patients show similar olfactory

291   impairments that those in AD[41]. In this sense, early olfactory deficits could lead to the

292   identification of depression patients with high risk of developing AD[41], as also occurs in our

293   APP/PSEN1-Tg animals by showing early depression-like behaviour with later hyposmia traits.

294   MD and AD are both associated with neuroinflammation and oxidative stress[11] and

295   evidence for the activation of both processes was observed in the differential expression analysis.

296   This show a dysregulation of inflammatory-related response genes, such as *Maml3*, *Zap70*, *Itgax*

297   and *App*[42–45] at both ages in APP/PSEN1-Tg mice. In addition, gene sets related to electron

298   transport chain are, in general, downregulated in APP/PSEN1-Tg animals at 6 months in PFC,

299   striatum and hippocampus, reflecting a possible abnormal function of mitochondrial metabolism,

300   as previously observed in AD[46] and MD[47].

301   One of the most striking observations is that majority of the negatively enriched gene sets

302   are associated with control of circadian rhythms, and these are observed in all brain areas of

303   interest (Figure 6B). In particular, we observe the downregulation of *Ciart* and *Dbp* in amygdala,

304   striatum and PFC at 3 and 6 months old (Figure 5 for more details). The expression of both genes

305   in anterior cingulate cortex modulates the circadian rhythms and mood[23,48], through the

306   MERK/ERK signalling pathway. Although disturbances in the circadian rhythms are associated

307   with both MD and AD[49], this is the first study in which both circadian transcripts are linked to

308   AD. A close relationship has been found between *Dbp* and AD, given that TGF-β2, present in the

309   cerebrospinal fluid of AD patients, inhibits the expression of some clock genes, including *Dbp*,

310   in *in vitro* assays. We also note that the predominant tau-kinase, reported to be downstream of β-

311   amyloid production[50–52], GSK3β, is a regulator of Per2 phosphorylation and hence a master-

312   regulator of the mammalian clock[53]. Our results suggest that there is a decline in the functional

313   control of circadian rhythms in APP/PSEN1-Tg mice that should be further studied in detail.

314   In summary, we suggest that MD could be an indicator of the early onset of AD. The

315   APP/PSEN1-Tg model of AD could recreate the early-depressive symptoms before developing

316   AD, as a prodromal stage of the neurodegenerative disease. In fact, this model provides *App*,

317   *Prnp*, *Ciart* and *Dbp* as possible shared biomarkers of AD and MD, despite the implications of

318   *App* and *Prnp* in MD remaining unclear[54–56]. In this sense, further studies combining post-mortem

319   human tissues of PFC, striatum, hippocampus and amygdala from AD patients with and without

320   an early history of depression, and transcriptomic analysis could help to provide additional

321   evidence on the combined biological signature of both diseases.

MATERIAL AND METHODS

323   See Supplementary material and methods for additional details.

Animals and rearing conditions

325   For the present study, we used 30 hemizygous double transgenic male mice (B6C3-Tg

326   (APPswe, PSEN1dD9)85Dbo/MmJax) model of AD (APP/PSEN1-Tg) and 30 male Non-

327   Transgenic control mice (004462, The Jackson Laboratory, USA). These transgenic mice express

328   a chimeric mouse/human APP (Mo/HuAPP695swe) and a mutant human presenilin-1 (PS1-dD9),

329   each controlled by independent mouse prion protein promoter elements[30]. The mice were

330   assigned to two different groups: APP/PSEN1-Tg and Non-Transgenic (n=16 per group) at 3

331   months-old, and APP/PSEN1-Tg and Non-Transgenic (n=14 per group) at 6 month-old, before

332   developing the β-amyloid plaques and right at onset[30]. All procedures were conducted in

333   accordance with national (BOE-2013-1337) and EU (Directive 2010-63EU) guidelines regulating

334   animal research and were approved by the local ethics committee (CEEA-PRBB).

11

335   *Behavioural Evaluation*

336   *Elevated plus maze* (EPM) (Panlab s.l.u, Barcelona, Spain) was performed using a black maze

337   elevated 30 cm above the ground[57]. Each mouse was placed in the centre of the maze, and was

338   allowed to freely explore for 5 min. The software SMART (Panlab s.l.u., Spain) automatically

339   recorded the number of entries and the time spent in the arms.

340   *Novel object recognition (NOR)*. Single trial NOR was performed in an open black arena (32 ×

341   28 cm) using 3 object types at opposite corners of the open field, 50 mm from the walls, similar

342   to those previously described[58]. Object exploration was defined as intentional contact between

343   the mouse's nose and the objects. The recognition index was defined as $[t_{Novel}/(t_{Novel} + t_{Familial})]$ x

344   100 for animals exploring novel objects in the acquisition trial.

345   *Left-right discrimination learning*. This test was performed using a T-maze apparatus, as

346   previously described[31]. This T-maze was filled with water (23 ± 1 °C). During the first two trials,

347   two identical platforms were submerged on the end of both arms to test possible side preferences.

348   A mouse was considered to have achieved criterion after 5 consecutive errorless trials. The

349   reversal-learning phase was then conducted 48h later, applying the same protocol except that mice

350   were trained to reach the escape platform of the opposite arm. Escape latencies and number of

351   trials to reach the criterion were manually recorded. A maximum of 20 trials were needed to

352   complete the experiment.

353   *Tail suspension test (TST)*. Each mouse was suspended individually 50 cm above a bench top for

354   6 min[57]. Mice were individually video-recorded and an observer, blind to the experimental

355   conditions, evaluated the percentage of time the animal was immobile during the test.

356   *Exposure to stress*. The stressful procedure consisted in the exposition to two mild stressful

357   situations each day during four consecutive days: animals were placed for 10 min in the open

358   field apparatus, and then they were placed in glass cylinders filled with water during 6 min.

359   Animals were subsequently evaluated for TST.

360   *Habituation-dishabituation test*. The test was performed as described[59]. After five minutes of

361   habituation to the cage, six consecutive one-minute presentations of a cotton swab with distilled

362   water were followed by one presentation of limonene (Sigma-Aldrich) solution 1:1000 in distilled

363   water. After that, five consecutive one-minute applications of distilled water were presented.

364   Tests were video-recorded and a blinded observer measured the time that mice spent sniffing the

365   cotton tip rearing on its hind limbs.

366   *Animal sacrifice and sample preparation for RNA extraction*

12

367   After behavioural analysis, animals were sacrificed by cervical dislocation and brains were

368   immediately removed from the skull. Brain samples were dissected at both ages: 3 and 6 months

369   old from Non-Transgenic and APP/PSEN1-Tg mice (n=6 per group). PFC (Figure 4I), striatum,

370   amygdala and hippocampus were dissected following an anatomical atlas[60]. Brain samples were

371   immediately stored at -80ºC until the RNA extraction. Then, each tissue sample was homogenized

372   in 1ml of QIAzol Lysis Reagent using a rotor–stator homogenizer (Polytron PT 2500 E;

373   Kinematica AG, Switzerland) during 20–40 seconds. After homogenization, the RNA was

374   extracted using RNeasy Lipid Tissue Mini Kit (Qiagen)[61].

375   *RNA sequencing*

376   *Library preparation and sequencing*

377   RNA samples (50-100 ng) with RIN scores from 7.6 to 9 (Agilent 4200 TapeStation)

378   were reverse transcribed to cDNA. Poly-A tail selection was done using Total Dual RNA-

379   Seq PolyA. cDNA was sequenced (HiSeq3000/4000) at the Oxford Wellcome Trust facility

380   obtaining 75 bp per read. On average, 33M reads were obtained per sample and a mapping rate

381   of ~85%.

382   *RNAseq DE analysis*

383   Raw sequencing reads in the 1710 paired fastq files were mapped with STAR version

384   2.5.3a[62] to the Gencode release 17 based on the GRCm38.p6 reference genome and using the

385   corresponding GTF file. The 885 bam files corresponding to 9 different lanes were merged for

386   each sample using Samtools 1.5, ending up with 95 bam files. The table of read counts was

387   obtained with featureCounts tool in subread package, version 1.5.1.

388   Further analyses were performed in R, version 3.4.3. Genes having less than 10 counts in

389   at least 10 samples were excluded from the analysis. Raw library size differences between

390   samples were treated with the weighted "trimmed mean method" TMM[63] implemented in the

391   edgeR package[64]. These normalized counts were used in order to make the unsupervised analysis,

392   heatmaps and clusters. For the differential expression (DE) analysis, read counts were converted

393   to log2-counts-per-million (logCPM), the mean-variance relationship was modelled with

394   precision weights using the voom approach and linear models were subsequently applied with

395   limma package, version 3.30.13[65] . p-values (p) were adjusted for multiple comparisons using the

396   Benjamini-Hochberg false discovery rate (FDR) approach. Genes were considered to be

397   differentially expressed if $|logFC|>0.585$ and adjusted $p<0.05$.

398   *qPCR validation*

399   Data were obtained from the qPCR platform using Taqman Low Density array (TLDA;

400   qPCR 7900HT, Life Technologies), where thirteen genes of interest were studied together with

401   the following endogenous controls: *Gapdh*, *Tbp* and *18S*. The gene *18S* was used to check overall

402   expression whereas *Gapdh* and *Tbp* were geometric averaged and included in posterior analyses

403   as the $C_t(endogenous)$. For each gene, DC_t was computed, comparing these values between

404   conditions. $DC_t = C_t(gene) - C_t(endogenous)$. Comparisons between studied conditions were

405   performed using a t-Student's t-test. Results were adjusted for multiple comparisons using the

406   FDR. The comparisons performed in each area are APP/PSEN1-Tg and Non-Transgenic at both

407   ages (validated genes in Supplementary Table 1).

408   *Functional and Pathway analysis*

409   Pre-ranked GSEA was used in order to retrieve enriched gene sets corresponding to functional

410   pathways[66]. The list of genes was ranked using the -log(p.val)*signFC value for each gene from

411   the statistics obtained in the DE analysis with limma.

412   For the gene set collection we used a database described previously[67] and available in

413   http://ge-lab.org/gs/. The gene sets in this database are harvested from different pathway data

414   sources and published studies all related to mice.

415   MGI genes IDs were converted to mouse symbol ID using the annotation files in

416   (http://www.informatics.jax.org/). As there were a high number of redundant gene sets in the

417   collection, a filtering strategy was applied to select the most representative ones. The filtering

418   steps were: i) pairwise Jaccard coefficients were computed between the gene sets from the

419   following data sources: Published articles, MPO, HPO, Reactome, MsigDB, GO_BP, KEGG,

420   PID, WikiPathways, INOH, PANTHER, NetPath, Biocarta, EHMN, MouseCyc and HumanCyc;

421   ii) for gene sets with a Jaccard = 1 (gene sets constituted by the same genes), only one was

422   considered, and iii) from gene sets with a Jaccard > 0.8, the gene set with the highest number of

423   genes was considered and the other gene sets were excluded from the gene set collection.

424   *DisGeNET database analysis*

425   We performed a GSEA to retrieve enriched gene sets associated with human diseases.

426   For this, we ranked the genes using the -log(p.val)*signFC value from the DE analysis. The gene

427   sets associated with human diseases, symptoms, and traits were retrieved from the DisGeNET

428   database (https://www.disgenet.org/, v7)[68]. DisGeNET integrates gene-disease associations

429   collected from curated repositories, from genome-wide association studies (GWAS) catalogues,

430   from animal models, and data obtained from the scientific literature using text mining

431   approaches[68]. For this analysis, we used only the curated gene sets in DisGeNET, that include

432   information from repositories such as UniProt, PsyGeNET, Clingen, and the Genomics England

433   Panel app. The mouse genes were converted to human gene IDs using the annotation files in

434   (http://www.informatics.jax.org/).

435   **STATISTICAL ANALYSIS**

436   For animal model experiments, analysis was performed using software SPSS 23.0 (SPSS

437   Inc., USA). Statistical differences were investigated by Student's t-test and ANOVA with

438   repeated measurement analysis. *Post-hoc* analysis was calculated with Bonferroni's correction

439   when applicable. Since habituation-dishabituation data were not normally distributed, Wilcoxon

440   matched-pairs rank test and Kruskal-Wallis test were calculated. Fisher's exact test was used to

441   evaluate differences in the percentage of animals that made an error in the Y-maze. For the GSEA

442   we only included those gene sets with a FDR q value<0.05 and |NES| >1.4.

443   **DATA AVAILABILITY**

444   The data that support the findings of this study are available from the corresponding author

445   upon reasonable request.

446

447

REFERENCES

1. World Health Organization. *Depression and Other Common Mental Disorders*. (2017).

2. Alexopoulos, G. S. *et al.* Executive dysfunction and long-term outcomes of geriatric depression. *Arch. Gen. Psychiatry* **57**, 285–290 (2000).

3. Potter, G. G., Kittinger, J. D., Wagner, H. R., Steffens, D. C. & Krishnan, K. R. R. Prefrontal neuropsychological predictors of treatment remission in late-life depression. *Neuropsychopharmacology* **29**, 2266–2271 (2004).

4. Ownby, R. L., Crocco, E., Acevedo, A., John, V. & Loewenstein, D. Depression and risk for Alzheimer disease: systematic review, meta-analysis, and metaregression analysis. *Arch. Gen. Psychiatry* **63**, 530–8 (2006).

5. Kaup, A. R. *et al.* Trajectories of Depressive Symptoms in Older Adults and Risk of Dementia. *JAMA psychiatry* **73**, 525–31 (2016).

6. Holmquist, S., Nordström, A. & Nordström, P. The association of depression with subsequent dementia diagnosis: A Swedish nationwide cohort study from 1964 to 2016. *PLOS Med.* **17**, e1003016 (2020).

7. van der Linde, R. M. *et al.* Longitudinal course of behavioural and psychological symptoms of dementia: systematic review. *Br. J. Psychiatry* **209**, 366–377 (2016).

8. Dorey, J. M. *et al.* Behavioral and psychological symptoms of dementia and bipolar spectrum disorders: Review of the evidence of a relationship and treatment implications. *CNS Spectrums* **13**, 796–803 (2008).

9. Dowlati, Y. *et al.* A Meta-Analysis of Cytokines in Major Depression. *Biol. Psychiatry* **67**, 446–457 (2010).

10. White, C. S., Lawrence, C. B., Brough, D. & Rivers-Auty, J. Inflammasomes as therapeutic targets for Alzheimer's disease. *Brain Pathol.* **27**, 223–234 (2017).

11. Rodrigues, R., Petersen, R. B. & Perry, G. Parallels between major depressive disorder and Alzheimer's disease: role of oxidative stress and genetic vulnerability. *Cell. Mol. Neurobiol.* **34**, 925–49 (2014).

12. Song, W. *et al.* Alzheimer's disease-associated TREM2 variants exhibit either decreased or increased ligand-dependent activation. *Alzheimer's Dement.* **13**, 381–387 (2017).

13. Pereira, A. C. *et al.* Age and Alzheimer's disease gene expression profiles reversed by the glutamate modulator riluzole. *Mol. Psychiatry* **22**, 296–305 (2017).

14. Klaassens, B. L., van Gerven, J. M. A., Klaassen, E. S., van der Grond, J. & Rombouts, S. A. R. B. Cholinergic and serotonergic modulation of resting state functional brain connectivity in Alzheimer's disease. *Neuroimage* **199**, 143–152 (2019).

15. Webster, S. J., Bachstetter, A. D., Nelson, P. T., Schmitt, F. A. & Van Eldik, L. J. Using mice to model Alzheimer's dementia: an overview of the clinical disease and the preclinical behavioral changes in 10 mouse models. *Front. Genet.* **5**, (2014).

16

485   16.   Du, Y. *et al.* MKP-1 reduces Aβ generation and alleviates cognitive impairments in
486   Alzheimer's disease models. *Signal Transduct. Target. Ther.* **4**, 58 (2019).

487   17.   Langa, K. M. & Levine, D. A. The diagnosis and management of mild cognitive
488   impairment: A clinical review. *JAMA - Journal of the American Medical Association*
489   **312**, 2551–2561 (2014).

490   18.   Correa, M. S. *et al.* Psychophysiological correlates of cognitive deficits in family
491   caregivers of patients with Alzheimer Disease. *Neuroscience* **286**, 371–382 (2015).

492   19.   Attems, J., Walker, L. & Jellinger, K. A. Olfactory bulb involvement in
493   neurodegenerative diseases. *Acta Neuropathol.* **127**, 459–75 (2014).

494   20.   Burrage, E., Marshall, K., Santanam, N. & Chantler, P. Cerebrovascular dysfunction
495   with stress and depression. *Brain Circ.* **4**, 43 (2018).

496   21.   Taylor, W. D., Aizenstein, H. J. & Alexopoulos, G. S. The vascular depression
497   hypothesis: Mechanisms linking vascular disease with depression. *Molecular Psychiatry*
498   **18**, 963–974 (2013).

499   22.   Satyanarayanan, S. K. *et al.* Melatonergic agonist regulates circadian clock genes and
500   peripheral inflammatory and neuroplasticity markers in patients with depression and
501   anxiety. *Brain. Behav. Immun.* **85**, 142–151 (2020).

502   23.   Li, J. Z. *et al.* Circadian patterns of gene expression in the human brain and disruption in
503   major depressive disorder. *Proc. Natl. Acad. Sci. U. S. A.* **110**, 9950–9955 (2013).

504   24.   Cao, X. *et al.* Astrocyte-derived ATP modulates depressive-like behaviors. *Nat. Med.* **19**,
505   773–777 (2013).

506   25.   Ganea, K. *et al.* Convergent animal and human evidence suggests the activin/inhibin
507   pathway to be involved in antidepressant response. *Transl. Psychiatry* **2**, e177 (2012).

508   26.   Chaki, S. & Okuyama, S. Involvement of melanocortin-4 receptor in anxiety and
509   depression. *Peptides* **26**, 1952–1964 (2005).

510   27.   Dean, B., Tsatsanis, A., Lam, L. Q., Scarr, E. & Duce, J. A. Changes in cortical protein
511   markers of iron transport with gender, major depressive disorder and suicide. *World J.*
512   *Biol. Psychiatry* 1–8 (2019). doi:10.1080/15622975.2018.1555377

513   28.   Watanabe, S. *et al.* Biological tests for major depressive disorder that involve leukocyte
514   gene expression assays. *J. Psychiatr. Res.* **66–67**, 1–6 (2015).

515   29.   Beckman, D. *et al.* Prion protein modulates monoaminergic systems and depressive-like
516   behavior in mice. *J. Biol. Chem.* **290**, 20488–20498 (2015).

517   30.   Jankowsky, J. L. *et al.* APP processing and amyloid deposition in mice haplo-
518   insufficient for presenilin 1. *Neurobiol. Aging* **25**, 885–892 (2004).

519   31.   Filali, M., Lalonde, R. & Rivest, S. Cognitive and non-cognitive behaviors in an
520   APPswe/PS1 bigenic model of Alzheimer's disease. *Genes, Brain Behav.* **8**, 143–148
521   (2009).

17

522 32. Mills, F. *et al.* Cognitive flexibility and long-term depression (LTD) are impaired
523   following β-catenin stabilization in vivo. *Proc. Natl. Acad. Sci. U. S. A.* **111**, 8631–6
524   (2014).

525 33. Bjartmar, L. *et al.* Long-term treatment with antidepressants, but not environmental
526   stimulation, induces expression of NP2 mRNA in hippocampus and medial habenula.
527   *Brain Res.* **1328**, 25–33 (2010).

528 34. Shen, Y. *et al.* Stimulation of the Hippocampal POMC/MC4R Circuit Alleviates
529   Synaptic Plasticity Impairment in an Alzheimer's Disease Model. *Cell Rep.* **17**, 1819–
530   1831 (2016).

531 35. Serova, L. I., Laukova, M., Alaluf, L. G. & Sabban, E. L. Blockage of melanocortin-4
532   receptors by intranasal HS014 attenuates single prolonged stress-triggered changes in
533   several brain regions. *J. Neurochem.* **131**, 825–835 (2014).

534 36. Goldman-Rakic, P. Cellular basis of working memory. *Neuron* **14**, 477–485 (1995).

535 37. Zhong, P. *et al.* Impaired Modulation of GABAergic Transmission by Muscarinic
536   Receptors in a Mouse Transgenic Model of Alzheimer's Disease. *J. Biol. Chem.* **278**,
537   26888–26896 (2003).

538 38. Chapman, P. F. *et al.* Impaired synaptic plasticity and learning in aged amyloid
539   precursor protein transgenic mice. *Nat. Neurosci.* **2**, 271–276 (1999).

540 39. Hsiao, K. *et al.* Correlative Memory Deficits, Aβ Elevation, and Amyloid Plaques in
541   Transgenic Mice. *Science (80-.).* **274**, 99–103 (1996).

542 40. Finnie, G. S. *et al.* Characterization of an 'Amyloid Only' Transgenic (B6C3-
543   Tg(APPswe,PSEN1dE9)85Dbo/Mmjax) Mouse Model of Alzheimer's Disease. *J.*
544   *Comp. Pathol.* **156**, 389–399 (2017).

545 41. Chen, B. *et al.* Cognitive Impairment and Structural Abnormalities in Late Life
546   Depression with Olfactory Identification Impairment: an Alzheimer's Disease-Like
547   Pattern. *Int. J. Neuropsychopharmacol.* **21**, 640–648 (2018).

548 42. Barger, S. W. & Harmon, A. D. Microglial activation by Alzheimer amyloid precursor
549   protein and modulation by apolipoprotein E. *Nature* **388**, 878–881 (1997).

550 43. Ho Kim, J. *et al.* Proteome-wide characterization of signalling interactions in the
551   hippocampal CA4/DG subfield of patients with Alzheimer's disease. *Sci. Rep.* **5**, 11138
552   (2015).

553 44. Nanus, D. E. *et al.* Regulation of the Inflammatory Synovial Fibroblast Phenotype by
554   Metastasis-Associated Lung Adenocarcinoma Transcript 1 Long Noncoding RNA in
555   Obese Patients With Osteoarthritis. *Arthritis Rheumatol.* **72**, 609–619 (2020).

556 45. He, W., Yuan, T. & Maedler, K. Macrophage-associated pro-inflammatory state in
557   human islets from obese individuals. *Nutr. Diabetes* **9**, 36 (2019).

558 46. Holper, L., Ben-Shachar, D. & Mann, J. Multivariate meta-analyses of mitochondrial
559   complex I and IV in major depressive disorder, bipolar disorder, schizophrenia,
560   Alzheimer disease, and Parkinson disease. *Neuropsychopharmacology* **44**, 837–849

561   (2019).

562   47.   Czarny, P., Wigner, P., Galecki, P. & Sliwinski, T. The interplay between inflammation,
563   oxidative stress, DNA damage, DNA repair and mitochondrial dysfunction in
564   depression. *Progress in Neuro-Psychopharmacology and Biological Psychiatry* **80**, 309–
565   321 (2018).

566   48.   Orozco-Solis, R. *et al.* A Circadian Genomic Signature Common to Ketamine and Sleep
567   Deprivation in the Anterior Cingulate Cortex. *Biol. Psychiatry* **82**, 351–360 (2017).

568   49.   Irwin, M. R. Sleep and inflammation: partners in sickness and in health. *Nat. Rev.*
569   *Immunol.* 1–14 (2019). doi:10.1038/s41577-019-0190-z

570   50.   Takashima, A. *et al.* Presenilin 1 associates with glycogen synthase kinase-3β and its
571   substrate tau. *Proc. Natl. Acad. Sci. U. S. A.* **95**, 9637–9641 (1998).

572   51.   Lovestone, S. *et al.* Alzheimer's disease-like phosphorylation of the microtubule-
573   associated protein tau by glycogen synthase kinase-3 in transfected mammalian cells.
574   *Curr. Biol.* **4**, 1077–1086 (1994).

575   52.   Hooper, C., Killick, R. & Lovestone, S. The GSK3 hypothesis of Alzheimer's disease.
576   *Journal of Neurochemistry* **104**, 1433–1439 (2008).

577   53.   Iitaka, C., Miyazaki, K., Akaike, T. & Ishida, N. A role for glycogen synthase kinase-3β
578   in the mammalian circadian clock. *J. Biol. Chem.* **280**, 29397–29402 (2005).

579   54.   Inoue, M. *et al.* Serum Levels of Albumin–β-Amyloid Complex in Patients with
580   Depression. *Am. J. Geriatr. Psychiatry* **24**, 764–772 (2016).

581   55.   Harrington, K. D., Lim, Y. Y., Gould, E. & Maruff, P. Amyloid-beta and depression in
582   healthy older adults: A systematic review. *Australian and New Zealand Journal of*
583   *Psychiatry* **49**, 36–46 (2015).

584   56.   Watanabe, S. Y. *et al.* Biological tests for major depressive disorder that involve
585   leukocyte gene expression assays. *J. Psychiatr. Res.* **66**–**67**, 1–6 (2015).

586   57.   Gracia-Rubio, I. *et al.* Maternal separation induces neuroinflammation and long-lasting
587   emotional alterations in mice. *Prog. Neuro-Psychopharmacology Biol. Psychiatry* **65**,
588   104–117 (2016).

589   58.   Montagud-Romero, S. *et al.* The novelty-seeking phenotype modulates the long-lasting
590   effects of intermittent ethanol administration during adolescence. *PLoS One* **9**, e92576
591   (2014).

592   59.   Agustín-Pavón, C., Martínez-Ricós, J., Martínez-García, F. & Lanuza, E. Role of nitric
593   oxide in pheromone-mediated intraspecific communication in mice. *Physiol. Behav.* **98**,
594   608–13 (2009).

595   60.   Paxinos, G. & Franklin, K. B. J. *The mouse brain in stereotaxic coordinates*. *Academic*
596   *Press* **2nd**, (2004).

597   61.   Lacinova, Z., Dolinkova, M., Haluzikova, D., Krajickova, J. & Haluzik, M. Comparison
598   of manual and automatic (MagNA Pure) isolation methods of total RNA from adipose

599   tissue. *Mol. Biotechnol.* **38**, 195–201 (2008).

600 62. Dobin, A. *et al.* STAR: ultrafast universal RNA-seq aligner. *Bioinformatics* **29**, 15–21
601   (2013).

602 63. Robinson, M. D. & Oshlack, A. A scaling normalization method for differential
603   expression analysis of RNA-seq data. *Genome Biol.* **11**, R25 (2010).

604 64. Robinson, M. D., McCarthy, D. J. & Smyth, G. K. edgeR: a Bioconductor package for
605   differential expression analysis of digital gene expression data. *Bioinformatics* **26**, 139–
606   40 (2010).

607 65. Smyth, G. K. limma: Linear Models for Microarray Data. in *Bioinformatics and*
608   *Computational Biology Solutions Using R and Bioconductor* 397–420 (Springer-Verlag,
609   2005). doi:10.1007/0-387-29362-0_23

610 66. Subramanian, A. *et al.* Gene set enrichment analysis: a knowledge-based approach for
611   interpreting genome-wide expression profiles. *Proc. Natl. Acad. Sci. U. S. A.* **102**,
612   15545–50 (2005).

613 67. Lai, L. *et al.* GSKB: A gene set database for pathway analysis in mouse. *bioRxiv* 082511
614   (2016). doi:10.1101/082511

615 68. Piñero, J. *et al.* The DisGeNET knowledge platform for disease genomics: 2019 update.
616   *Nucleic Acids Res.* **48**, D845–D855 (2020).

617

FUNDING AND DISCLOSURE

AKNOWLEDGEMENTS

AUTHOR CONTRIBUTIONS

A.M-S, L.N, L.I.F., F.S. and O.V. were responsible for the study concept and design. A.M-S. performed behavioural studies. A.M-S, E.M.R., A.H.N. and S.L. contributed to transcriptomic analysis. J.P., M.A., L.N., F.S. and L.I. F. carried out the bioinformatics analysis. All the authors participated in the interpretation of findings. A.M-S., F.S., and O.V. drafted the manuscript. All authors critically reviewed the content and approved the final version for publication.

CONFLICTS OF INTEREST

The authors declare no conflicts of interest regarding the work presented here.

643 **FIGURES**
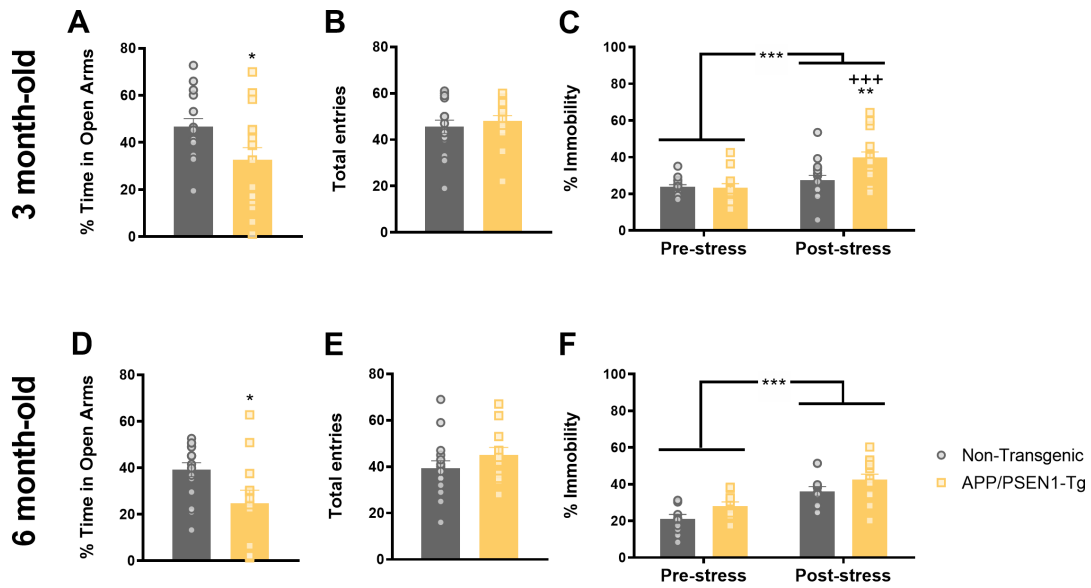
644
645 *Figure 1. APP/PSEN1-Tg animals show early anxiety-like and despair-like behaviours induced by stress.*
646 Panels A,B,D and E represent the EPM results, and panels C and F correspond to the TST results. Grey (Non-
647 Transgenic) and yellow (APP/PSEN1-Tg) bars represent the percentage of time spent in open arms (A, D) and total
648 number of entries (B,E) at 3 (n=16 per group) and 6 months (n=14 per group). (*p < 0.05, Student's t-test Non-
649 Transgenic *vs* APP/PSEN1-Tg). Grey (Non-Transgenic) and yellow (APP/PSEN1-Tg) bars represent the percentage of
650 time that animals are immobile in TST at 3 (n=16 per group) (C) and 6 months-old (Non-Transgenic n=12,
651 APP/PSEN1-Tg n=14) (F) in pre-stress and post-stress conditions. Data are presented as mean ± SEM. ***p<0.001
652 Pre-stress *vs* post-stress condition; +++ p<0.001 comparison APP/PSEN1-Tg pre-stress *vs* post-stress, **p<0.01
653 comparison APP/PSEN1-Tg *vs* Non-Transgenic post-stress condition. (two-way ANOVA).
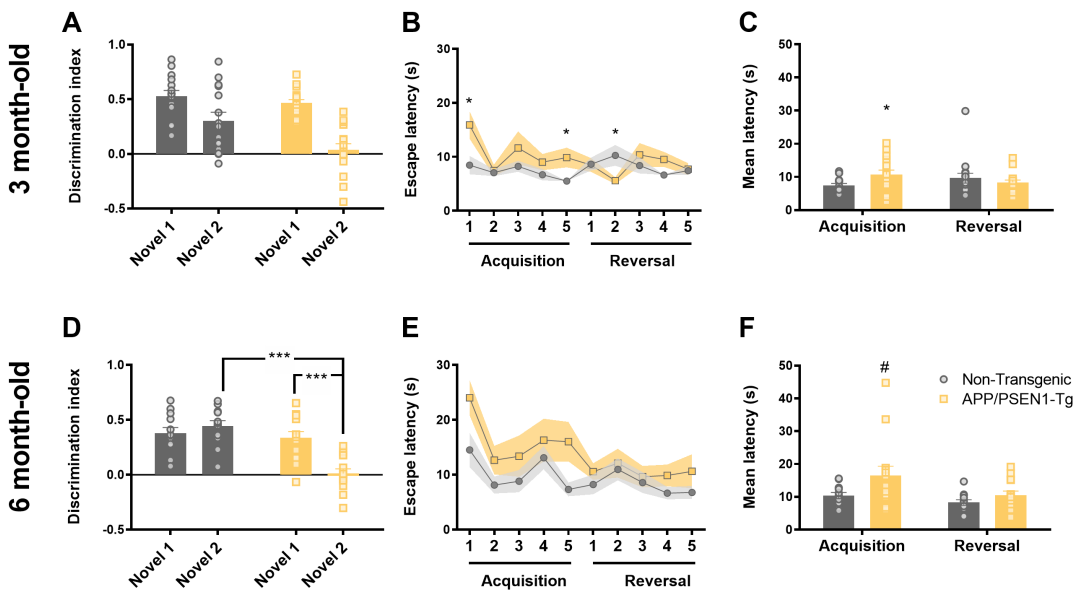

654

655 *Figure 2. The onset of memory impairments in APP/PSEN1-Tg occurs at 3months-old.*

22

656 Novel object recognition test: Grey (Non-Transgenic) and yellow (APP/PSEN1-Tg) bars represent the novel object 1
657 and 2 discrimination index (%) at 3 (A) (Non-Transgenic n=15, APP/PSEN1-Tg n=16) and 6 months old (D) (Non-
658 Transgenic n=12, APP/PSEN1-Tg n=14). Data are presented as mean ± SEM. *p<0.05, **p < 0.01 (two-way ANOVA).
659 T-maze left-right discrimination learning: (B, E) Solid (Non-Transgenic) and dotted line (APP/PSEN1-Tg) represent
660 the escape latencies of both groups at two different ages. (ANOVA of repeated measurements *p<0.05; +p<0.05
661 comparison APP/PSEN1-Tg *vs* the 1st trial; *p<0.05 comparison APP/PSEN1-Tg *vs* Non-Transgenic). (C, F) Grey
662 (Non-Transgenic) and yellow (APP/PSEN1-Tg) bars represent the mean ± SEM trials to criterion during acquisition
663 and reversal phases latencies at 3 (n=16 per group) and 6 months-old (Non-Transgenic, n=12, APP/PSEN1-Tg n=14).
664 (F) At 6 months-old, transgenic mice tend to reach the criterion later than control groups during acquisition. (Student's
665 t-test, Non-Transgenic *vs* APP/PSEN1-Tg, *p<0.05; #p=0.068).
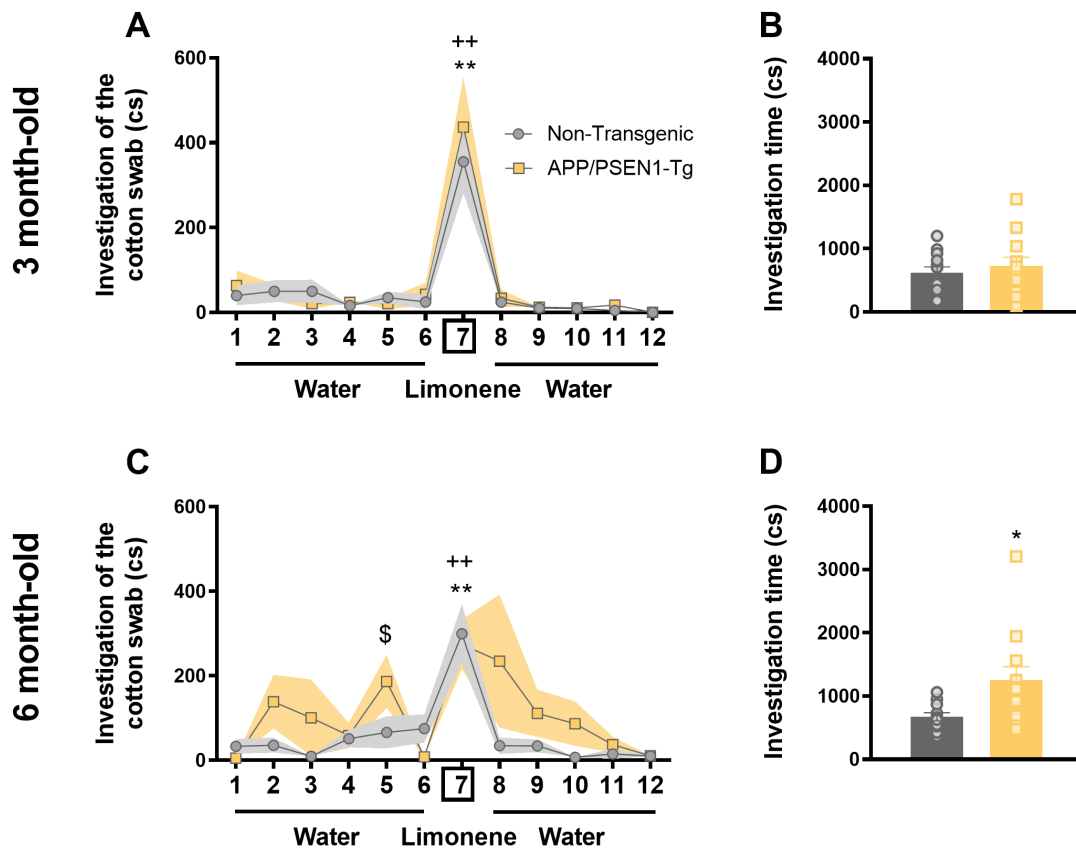
666
667 *Figure 3. APP/PSEN1-Tg mice show olfaction disruptions at 6 months old.*
668 Graphs show the time (centiseconds, cs) that APP/PSEN1-Tg and Non-Transgenic animals spent investigating a cotton
669 swab through consecutive one-minute presentations (mean± SEM) of distilled water (presentations 1-6 and 8-12) and
670 limonene (presentation 7) at 3 (A) and 6 months (C). The exploration time during the first presentation of the cotton
671 swab with water [1] was compared with that of the first presentation of limonene [7] in each group. (Wilcoxon test,
672 **p<0.01 comparison APP/PSEN1-Tg water *vs* limonene presentations; ++p<0.01 comparison Non-Transgenic water
673 *vs* limonene presentations; Kruskal-Wallis test $p<0.05 comparison APP/PSEN1-Tg *vs* Non-Transgenic). Grey (Non-
674 Transgenic) and yellow (APP/PSEN1-Tg) bars represent the total investigation time at (B) 3 (n=12 per group) and 6
675 (D) months old (Non-Transgenic n=11, APP/PSEN1-Tg n=12) (Student's t-test *p<0.05). Data are presented as mean
676 ± SEM.

677

678

679
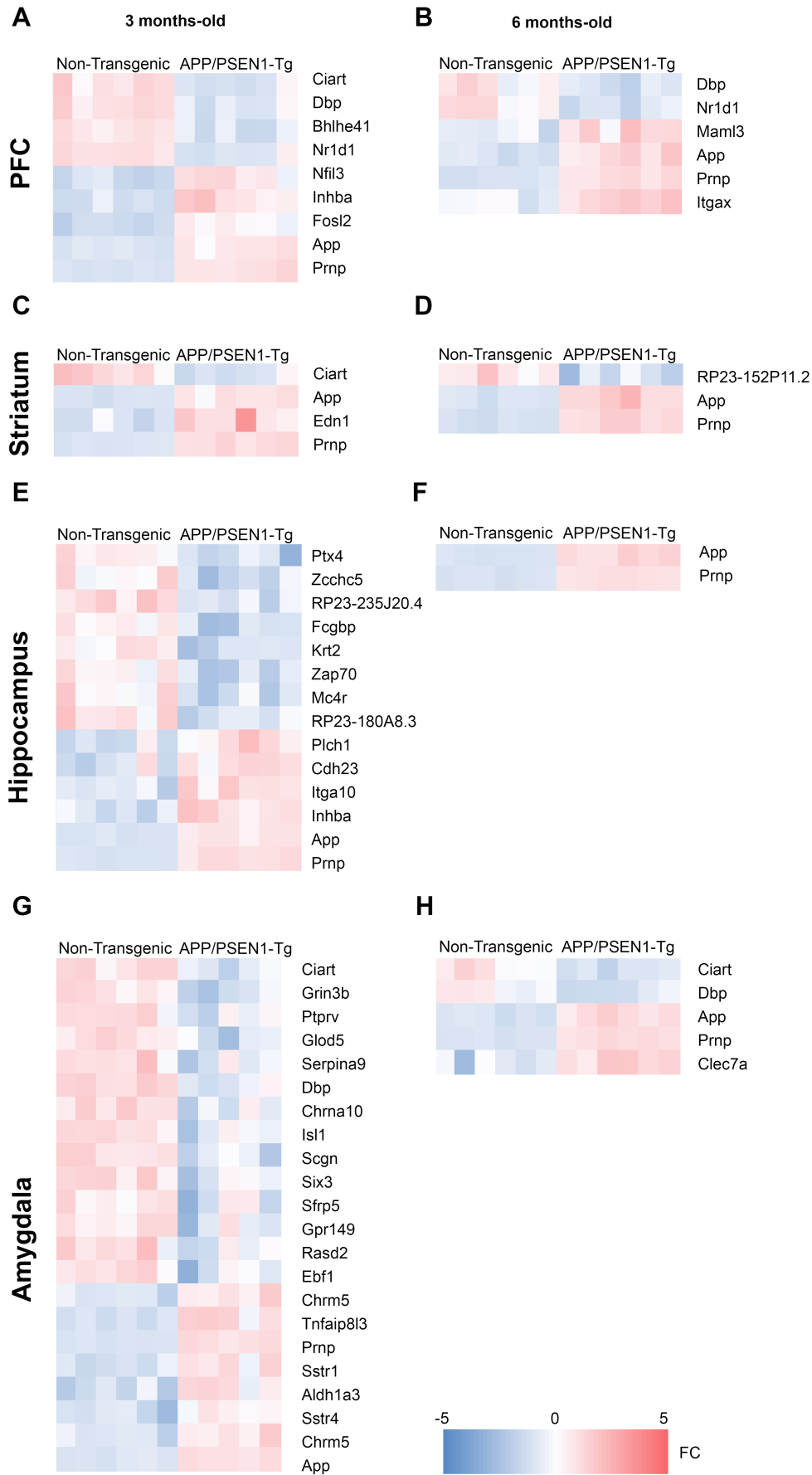
680 *Figure 4. Differentially expressed genes in the PFC, striatum, hippocampus and amygdala from APP/PSEN1-Tg*

681 *mice at 3 and 6 months-old.*

682 Heatmaps representing the degree of change for the differentially expressed genes at 3 (A,C,E,G) and 6 (B,D,F,H)

683 months between control and APP/PSEN1-Tg (5-6 independent brain samples per area). (G) The heatmap from

684 amygdala at 3 month-old is a reduced representation from >100 up and downregulated genes (p < 0.05; |logFC| >0.59).

685 Legend (bottom) indicates the color-coded fold-change scale (-5<FC<5) where negative values represen

686 downregulation in blue, and positive upregulation in red.
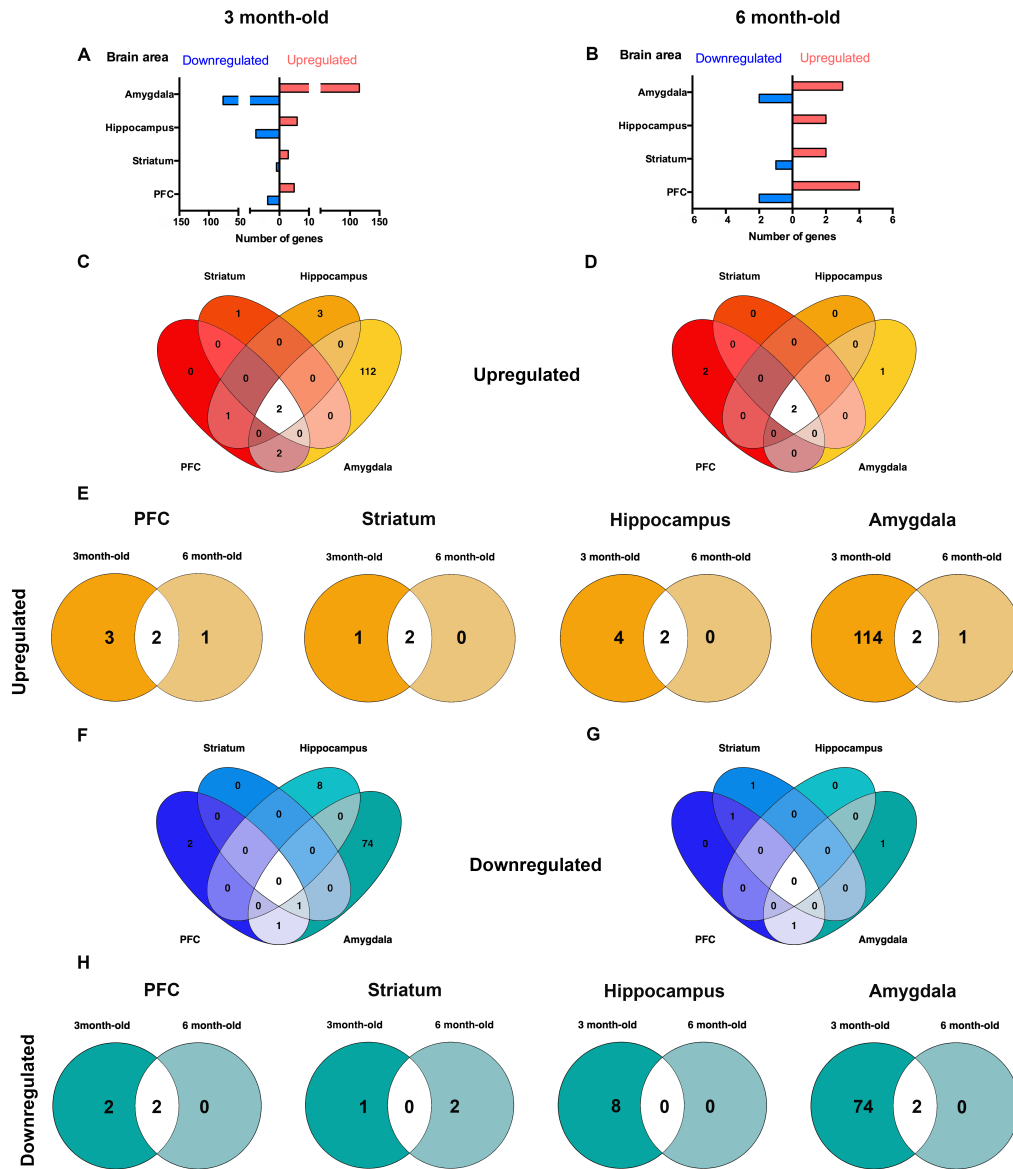
687
688 *Figure 5. Distribution pattern of differentially expressed genes from APP/PSEN1-Tg mice model.*

689 Total number of up (red bars) and downregulated (blue bars) genes within amygdala, hippocampus, striatum and PFC

690 at (A) 3 months and (B) 6 months. Venn diagrams show the number of differentially expressed genes among areas, in

691 an upregulated (C,D) and downregulated (F,G) way. Venn diagrams show the number of upregulated (E) and

692 downregulated (H) shared genes between 3 and 6 months old of age APP/PSEN1-Tg (n=6 per group) *vs* Non-

693 Transgenic mice (n=6 per group).

25
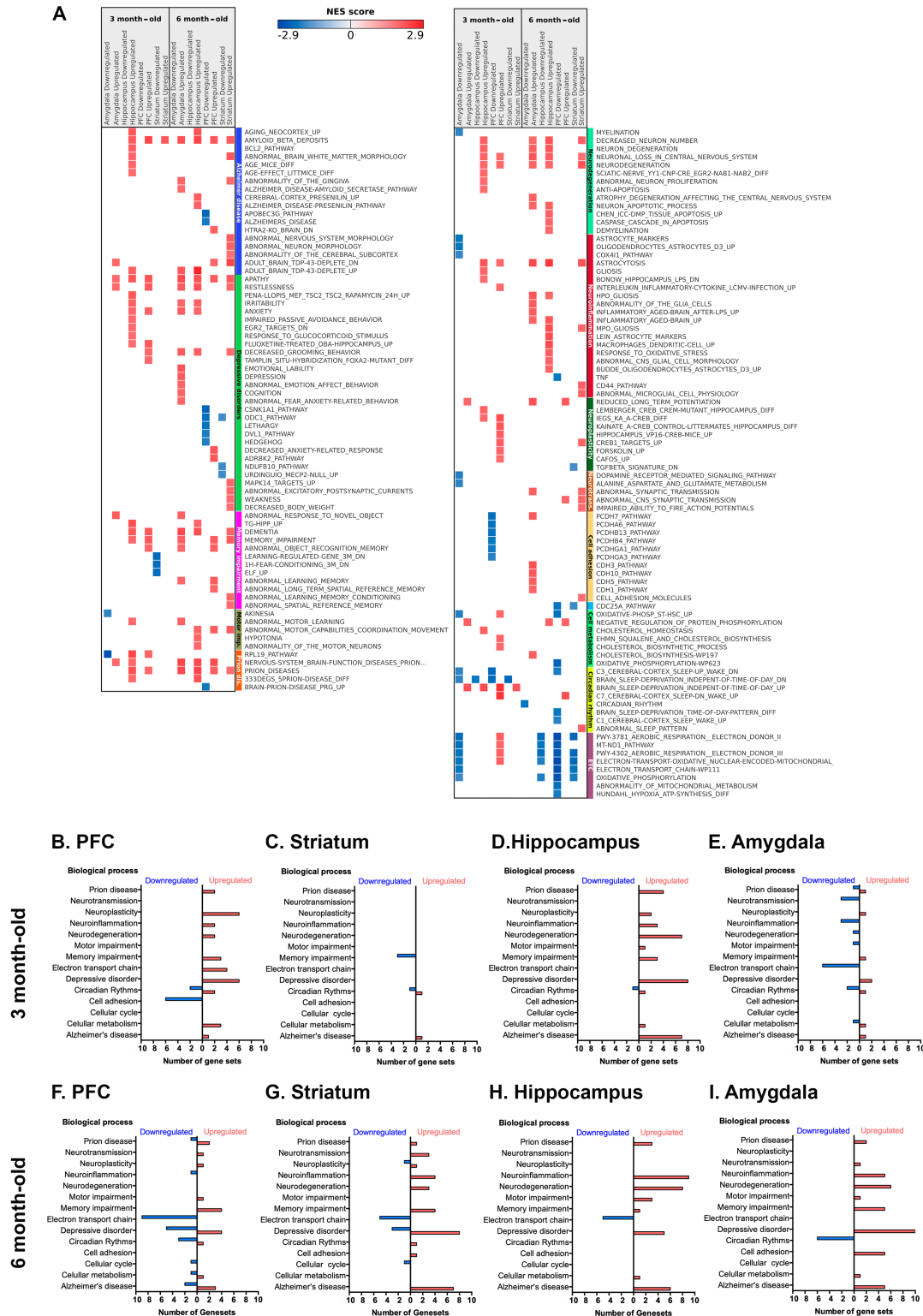
Figure 6. Comparison of differentially expressed gene sets in APP/PSEN1-Tg mice in PFC, striatum, hippocampus and amygdala.

(A) The heatmap represents some selected up and downregulated gene sets at 3 and 6 month-old included in different biological processes: Alzheimer disease, depressive disorders, memory impairment, prion disease, motor impairment (Motor imp.), neurodegeneration, neuroinflammation, neuroplasticity, neurotransmission (Neurotrans.), cell adhesion, circadian rhythm, electronic transport chain (ETC). (FDR q value <0.05; |NES| >1.4.). List of the total number of differentially expressed gene sets ordered by biological processes found in PFC (B,F), striatum (C,G), hippocampus (D,G) and amygdala (E,J) at 3 and 6 months old, respectively. Red bars (positive) represent the upregulated expressed

26

703   gene sets and the blue bars (negative) show downregulated gene sets in each area. For the GSEA we only included

704   those gene sets with FDR q value <0.05 and |NES| >1.4.

705